Original Article

DOI: 10.14235/bas.galenos.2025.26121
Bezmialem Science 2026;14(3):220-232

β-sitosterol, A Potential Enzyme Inhibitor Molecule From *Nepeta* Species: *In vitro* and *In silico* Approaches

Nepeta Türlerinden Elde Edilen Potansiyel Bir Enzim Inhibitörü Molekülü β-sitosterol: *In vitro* ve *In silico* Yaklaşımlar

Semiha YENİGÜN[1], Yunus BAŞAR[2], Yaşar IPEK[3], İbrahim DEMİRTAŞ[4], Tevfik OZEN[1], Lütfi BEHCET[5]

[1]Ondokuz Mayıs University Faculty of Sciences, Department of Chemistry, Samsun, Türkiye
[2]Iğdır University Scientific Research Projects Coordination Unit, Iğdır, Türkiye
[3]Çankırı Karatekin University Faculty of Science, Department of Chemistry, Çankırı, Türkiye
[4]Ondokuz Mayıs University Faculty of Pharmacy, Department of Pharmaceutical Chemistry, Samsun, Türkiye
[5]Bingöl University Faculty of Arts and Sciences, Department of Molecular Biology and Genetics, Bingöl, Türkiye

ABSTRACT

Objective: In the literature, β-sitosterol (BS), one of the primary phytosterol components found in plant-based dietary sources, has been reported to exhibit antidiabetic, antimicrobial, enzyme-inhibiting, anti-inflammatory, antioxidant, trypanocidal, anticancer, and antinociceptive effects. Therefore, in our present study, we aimed to isolate BS from the genus *Nepeta* (*N. trachonitica*, *N. aristata*, *N. italica*, *N. baytopii*, and *N. stenantha*) using column chromatography (silica gel) and to elucidate BS using chromatographic methods (NMR and MS).

Methods: Detailed studies (*in vitro* and *in silico*) were conducted on metabolic enzymes (carbonic anhydrase, tyrosinase, α-amylase, urease, α-glucosidase, and lipase) of BS, isolated as the main component from five different *Nepeta* species, and statistically compared with standard drugs.

Results: It was observed that BS had effective inhibitory effects when compared with standard drugs in inhibiting urease (IC_{50}, 21.60±0.01 μM) and tyrosinase (IC_{50}, 6.60±0.02 μM). In kinetic studies, BS was found to have an effective inhibitory capacity on α-glucosidase with an inhibitory constant of 25.67 μM. BS was found to have a high binding affinity with tyrosinase in molecular docking. In addition, the complex of tyrosinase and BS, which had not undergone molecular dynamics simulation

ÖZ

Amaç: Literatürde, bitki bazlı besin kaynaklarının temel fitosterol bileşenlerinden biri olan β-sitosterolün (BS), antidiyabetik, antimikrobiyal, enzim inhibitörü, antienflamatuvar, antioksidan, tripanosidal, antikanser ve antinosiseptif etkilere sahip olduğu bildirilmiştir. Bu nedenle, mevcut çalışmamızda BS, *Nepeta* cinsinden (*N. trachonitica, N. aristata, N. italica, N. baytopii* ve *N. stenantha*) kolon kromatografisi (silika jel) kullanılarak izole edilmesi ve BS'nin kromatografik yöntemler (NMR ve MS) kullanılarak aydınlatılması amaçlanmıştır.

Yöntemler: Beş farklı *Nepeta* türünden ana bileşen olarak izole edilen BS'nin metabolik enzimleri (karbonik anhidraz, tirozinaz, α-amilaz, üreaz, α-glukozidaz, lipaz) üzerinde detaylı çalışmalar (*in vitro* ve *in silico*) yürütülmüş, standart ilaçlarla istatistiksel olarak karşılaştırılmıştır.

Bulgular: BS standart ilaçlarla karşılaştırıldığında üreazı (IC_{50}, 21,60±0,01 μM) ve tirozinazı (IC_{50}, 6,60±0,02 μM) inhibe etmede güçlü inhibitör etkilere sahip olduğu gözlenmiştir. Kinetik çalışmalarda, BS'nin 25,67 μM'lik bir inhibitör sabiti ile α-glukozidaz üzerinde etkili bir inhibitör kapasitesine sahip olduğu bulunmuştur. BS'nin moleküler yerleştirmede tirozinaz ile yüksek bağlanma afinitesine sahip olduğu bulunmuştur. Ayrıca, daha önceki çalışmalarda moleküler dinamik

Address for Correspondence: Prof. Dr., Tevfik Ozen, Ondokuz Mayıs University Faculty of Sciences, Department of Chemistry, Samsun, Türkiye
E-mail: tevfikoz@omu.edu.tr
ORCID IDs of the authors: S.Y.: 0000-0002-1979-5427, Y.B.: 0000-0002-7785-3242, Y.I.: 0000-0002-1041-267X, İ.D.: 0000-0001-8946-647X, T.O.: 0000-0003-0133-5630, L.B.: 0000-0001-8334-7816

Cite this article as: Yenigün S, Başar Y, İpek Y, Demirtaş I, Ozen T, Behcet L. β-sitosterol, a potential enzyme inhibitor molecule from *Nepeta* species: *in vitro* and *in silico* approaches. Bezmialem Science. 2026;14(3):220-232

Received: 23.07.2025
Accepted: 24.12.2025
Published date: 22.07.2026

ABSTRACT

in previous studies, reached stability at 4 nm in the RMSD graph, and the binding energy was recorded as -4.39 kcal/mol in the MM/PBSA analysis.

Conclusion: The *in silico* results supported that *Nepeta* species and BS are effective on the dermatological enzyme (tyrosinase) and may be candidates for a new dermatological product.

Keywords: *Nepeta* species, β-sitosterol, *in vitro* activities, *in silico* studies

ÖZ

simülasyonu yapılmayan tirozinaz ve BS kompleksi, RMSD grafiğinde 4 nm'de kararlılığa ulaşmış ve bağlanma enerjisi MM/PBSA analizinde -4,39 kcal/mol olarak kaydedilmiştir.

Sonuç: *In silico* sonuçlar, *Nepeta* türlerinin ve BS'nin dermatolojik enzim (tirozinaz) üzerinde etkili olduğunu ve yeni bir dermatolojik ürün adayı olabileceğini desteklemektedir.

Anahtar Kelimeler: *Nepeta* türleri, β-sitosterol, *in vitro* aktiviteler, *in silico* çalışmalar

Introduction

Plants produce phytochemicals to facilitate environmental adaptation, resist stress conditions, ensure survival, and provide chemical defense against insects and harmful microorganisms. Phytochemicals can be divided into phenols, alkaloids, and terpenes (1). These compounds exhibit diverse biological properties, including antioxidant activity, antimicrobial effects, enzyme inhibition, and immune system stimulation (2). The Lamiaceae family is represented in the flora of Türkiye by 45 genera, 565 species, and 735 taxa. *Nepeta*, one of the most abundant genera of the Lamiaceae family, includes 34 species and 40 taxa in Türkiye (3). *Nepeta* species have rich content in terms of nepetalactone, diterpene, triterpene, sesquiterpene, and iridoids (4).

Triterpenes, a group of natural compounds, are transformed into metabolites such as saponins, steroids, and sterols in the cell (5). Phytosterols are a subgroup of steroids, a class of important bioorganic molecules widely distributed in fungi, plants, and animals (6). It is structurally similar to cholesterol. The European Food Safety Authority recommends consuming approximately 1.5-2.4 g of phytosterols per day to lower blood cholesterol levels. At the same time, the Food and Drug Administration states that the role of sterol/phytosterol is at least 1.3 g/day in reducing the risk of heart disease (6). Stigmasterol, campesterol, and β-sitosterol (BS) are the dominant phytosterols in human herbal nutrition. BS has antidiabetic, antimicrobial, enzyme-inhibiting, anti-inflammatory, antioxidant, anticancer, trypanocidal, and antinociceptive effects (7). It is also used as an antidote against snake venom (6).

The Norwegian Food Safety Authority says BS can be used in sunscreens, moisturizers, body washes, and anti-aging cosmetics due to its skin-regulating effect (8). In one study, BS was reported to block the production and messenger RNA expression of thymic stromal lymphopoietin by inhibiting the caspase-1 and nuclear factor-kB signaling pathways in the stimulated human mast cell line HMC-1 cells (9). It is known that various plant species containing phytosterols have been used for centuries to treat wounds and skin burns (8). In a study conducted in mice, BS reduced clinical symptoms such as eczema, dryness, and erythema, serum histamine, and immunoglobulin E levels in 2,4-dinitrochlorobenzene-induced atopic dermatitis and histamine-induced itching. BS was found to inhibit the expression of interleukin-6 in atopic dermatitis-like skin lesions and HaCaT cells (10).

Biological macromolecules, which are considered the main components of drugs used in treating diseases, contribute to the treatment by inhibiting enzymes. Recently, enzyme inhibitors accounted for almost half of the drugs used for clinical purposes. Research on the human genome reveals that enzymes predominate in the disease-relevant regions that code for the targets to which drugs are directed. Future pharmacological research is expected to continue to concentrate on precise enzyme inhibition. For this reason, enzymes have recently become the target of major pharmaceutical and biotechnology companies' efforts in discovering and developing new drugs (11). *In silico* studies are conducted to support experimental investigations of the interaction between enzymes and molecules in a computer environment. This provides time and economic advantages.

For this purpose, the enzyme inhibitory activities (urease, carbonic anhydrase (CA), tyrosinase, lipase, α-amylase, and α-glucosidase) of BS isolated from the *Nepeta* genus (*N. trachonitica, N. aristata, N. italica, N. baytopii,* and *N. stenantha*) were determined. Enzyme kinetics, molecular dynamics (MD), molecular docking, and molecular mechanics Poisson-Boltzmann surface area (MM/PBSA) analysis were investigated. In this study, inhibition of urease, CA, lipase, and tyrosinase, and inhibition kinetics of these enzymes and the complex of tyrosinase enzyme and BS, which did not have an MD simulation, and MM/PBSA analysis in previous studies, were investigated for the first time. The study aims to provide new perspectives on the existing literature by conducting further research on BS, which is known to have high activity.

Methods

Collection of Plant Material and Extraction of the *Nepeta* Genus

N. aristata Boiss. & Kotschy (BIN6195, Endemic), *N. baytopii* Hedge & Lamond (BIN5933, Endemic), *N. italica* L. (BIN7496), *N. stenantha* Kotschy & Boiss., and *N. trachonitica* Post (BIN7722) were collected and identified by Prof. Dr. Lütfi Behçet. The plants were deposited in the herbarium of Bingöl University, Türkiye.

The aerial parts of five *Nepeta* species were ground, dried, and extracted using a chloroform: methanol (1:1) mixture. This extraction was repeated three times. The extracts were filtered through filter paper (Whatman No. 1). The solvent in the extract was removed using a rotary evaporator. The extracts were then dried and stored for use in activities after being lyophilized. The crude extracts were fractionated by column chromatography using a silica gel column with increasing solvent polarity. Various subfractions were obtained in silica gel 60 and Sephadex LH-20 columns. Similar fractions were analyzed using the TLC profile, merged to save time and consumables, and the number of fractions decreased.

Fraction and Isolation

Extracts were separated on the column (silica gel) by changing the solvent from low polarity to high polarity. Various subfractions of the fractions were obtained using silica gel and the Sephadex column. Similar fractions were analyzed using TLC profiling, merged to save time and consumables, and the number of fractions was decreased. BS was isolated using column chromatography (silica gel) as follows; *N. baytopii* from the first fraction of the chloroform extract, *N. italica* from the first fraction of the chloroform extract using Sephadex LH20 column chromatography; *N. aristata* from the fifth fraction of the chloroform extract, *N. stenantha* from the third fraction of the chloroform extract, and *N. trachonitica* from the sixth fraction of the chloroform extract.

Nuclear Magnetic Resonance (NMR) Spectroscopy Analysis

The NMR spectrometer was used to get the ^{13}C (Agilent at 150 MHz) and ^{1}H (Agilent at 600 MHz) NMR spectra of samples in CD_3OD to determine the molecule's structure. Additionally, three different 2D NMR spectra were utilized with COSY, HSQC, and HMBC (11,12).

Mass Spectrometry (MS)

An MS integrated with an Agilent 6460 Triple Quad brand liquid chromatography (HPLC) system was used to confirm the BS's mass, whose structure was determined. After the analytical column was taken out, the eluent (acetonitrile + ammonium formate and formic acid) was added. It was performed with a 4 µL injection volume and a 0.400 mL/min solvent flow. The application was completed in a total of 120 seconds in the 50-1200 m/z scanning range. MS spectra were generated as a result of the specified adjustments (13).

Enzyme Kinetics and Inhibitions

Inhibitions of BS with urease (14), CA (15), tyrosinase (16), α-amylase (17), α-glucosidase (18), and lipase (19) enzymes, as well as inhibition categories and binding constants, were determined spectrophotometrically using the BIOTEK (Epoch 2) microplate reader. The inhibition findings were used to calculate half-maximal drug inhibitory concentration (IC_{50}) values (µg/mL) of all inhibition results. Michaelis-Menten and Lineweaver-Burk graphs were made with varying quantities and substrates to ascertain the enzyme's kinetics. BS's inhibitor constant (K_i) was calculated using the V_{max} and K_m values from the Lineweaver-Burk chart (11).

Molecular Interaction Applications

Chem Draw Ultra 18.0 was used to draw the BS structure, and Chem3D 18.0 was used to compute the lowest energy. The enzymes used in our tests, which were selected from the protein database (RCSB PDB: Homepage), utilized 3D protein structures. α-amylase from porcine pancreas (1OSE), urease from Jack bean (4GY7), lipase from porcine pancreas (1HPL), α-glucosidase from *Saccharomyces cerevisiae* (3AJ7), CA from Bovine erythrocytes (3HS4), tyrosinase from mushroom (5M6B) were selected. To determine the interaction of the molecule with the active site of the enzymes. 2D and 3D images and data of the structure formed by the compound and the enzyme were taken using the Discovery Studio program. Based on the binding affinities, the binding constants (K_i) and the binding affinities were calculated in Excel (3,20).

MD Simulations and MM/PBSA Analysis

The MD simulation used BS's interactions with highly active enzymes within 100 ns to examine its dynamic mobility. GROMACS software was utilized for this simulation. Conducted utilizing the TIP3P water dissolving method in conjunction with the force field (Charmm36-July-2022) at 310 K. To neutralize the system and equalize the charge, ions (Na^+ and Cl^-) were added. Ligand topology was generated via the CGenFF server. After the NVT step, the temperature is increased to 310 K by integrating the temperature using a 100-ps V scale. The system was further stabilized by positional restraint of the backbone atoms using the Parrinello-Rahman barostat with NPT and a coupling constant of 0.1 ps. After the adjustments were completed, the MD simulation was run for 100 ns. Along the way, the integrated GROMACS software tools were used to examine the hydrogen bonding, root-mean-square fluctuation (RMSF), radius of gyration (Rg), and root mean square deviation (RMSD). The charts were generated using GRACE software. The MM/PBSA method was used to calculate the complex's binding free energy.The "gmx_

mmpbsa" tool was used to determine the binding free energies for each complex (20,21).

Statistical Analysis

The findings of *in vitro* tests were used to calculate biological activity ± standard deviations. For statistical parameters, the IBM SPSS 20.0 software was utilized, and an analysis of variance test was used. Based on the multiple comparison analysis results, the Tukey HSD[a,b] test was used. Statistical significance was expressed as $p<0.05$.

Results

In the silica gel column, plant extracts were divided into fractions based on increasing solvent polarity (*n*-hexane, chloroform, ethyl acetate, and methanol). The resulting fractions were divided into subfractions in a silica gel 60 and a Sephadex LH-20 column. Accordingly, the BS molecule was isolated from *N. aristata* (Fr5 in Sephadex column), *N. stenantha* (Fr3 in Sephadex column), *N. trachonitica* (Fr6 in sephadex column), *N. baytopii* (Fr1 in the silica-gel column), and *N. italica* (Fr1 in the silica-gel column) (Figure 1).

Structural Analysis of BS by NMR Techniques

In the structure determination of BS, as a result of ^{1}H-NMR analysis, complex signals in the aliphatic region revealed that the molecule was a phytosterol. Accordingly, the specific olefinic signal at 5.34 ppm indicated the presence of a double bond in the structure. The signals in the 0.6-1.2 ppm range indicated the presence of methyl groups, and the signal at 3.51 ppm confirmed that the oxygen atom was bonded. When the COSY interactions of the signals at 2.25-2.28 ppm were examined, it was observed that these signals indicated the -CH2 group was adjacent to an electronegative region. Examination of HSQC and HMBC interactions, as well as a comparison of ^{1}H- and ^{13}C-NMR data from the literature, confirmed that the structure is BS (Figure 2 and Table 1) (22). The molecule has the chemical formula $C_{29}H_{50}O$. Its (m/z) mass was calculated to be 414.71 negative ion/mass and confirmed with literature information.

Enzyme Inhibitions and Kinetic Assays

All living cells use enzymes to catalyze reactions in various biological functions. Because modifying enzyme function yields precise and rapid consequences, enzymes remain the primary targets for drug development. Even while the number of medications used to alter extracellular signaling receptors is growing, 47% of the medications on the market now block enzyme targets (23).

Studies were conducted on BS's urease, CA, tyrosinase, lipase, α-amylase, and α-glucosidase enzymes. Lineweaver-Burk plots of the inhibition kinetics of BS with enzymes are shown in Figure 3. Compared with the standards used in enzymes, it was determined that BS showed high efficacy in urease and tyrosinase inhibition (Table 2).

Molecular Docking

Five alkyl contacts with ARG439, ALA440, MET588, and MET637, as well as four pi-alkyl (P-A) interactions with HIS492 and HIS519, were found for BS, which interacts with

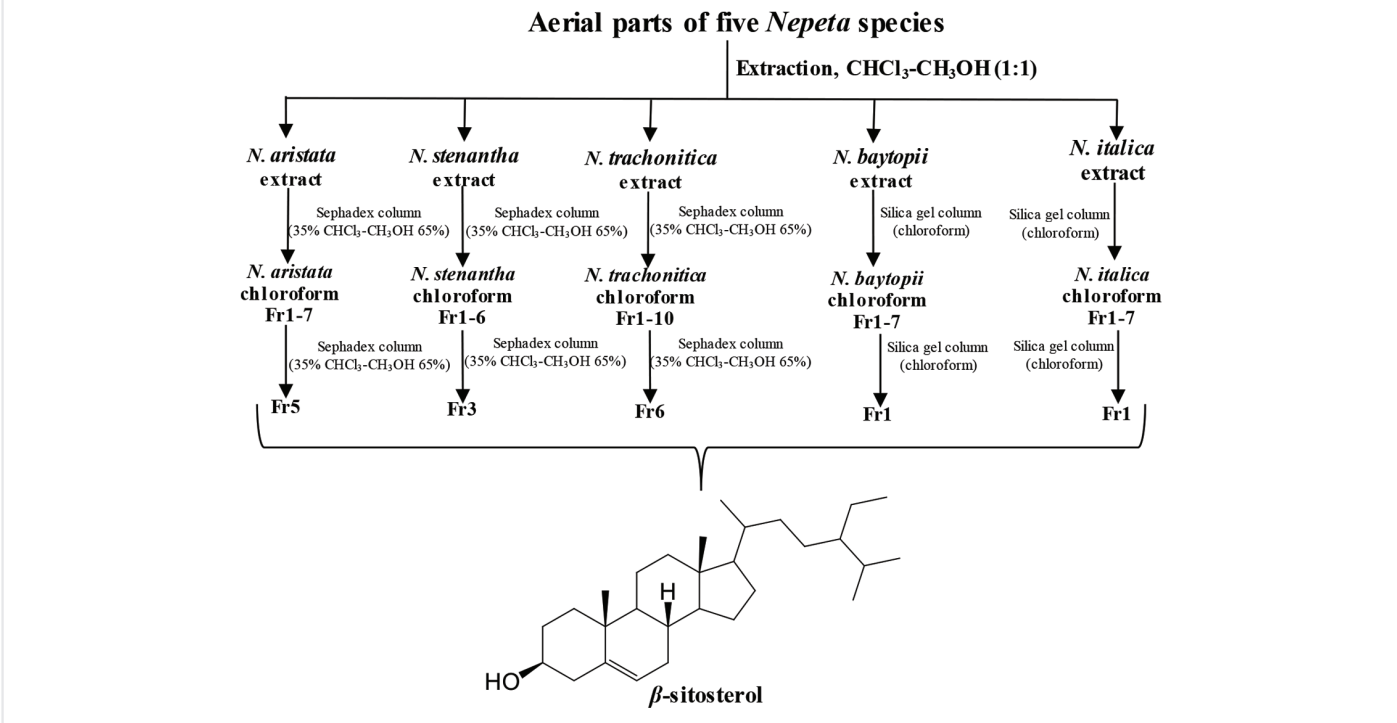

Figure 1. Scheme of isolation of the β-sitosterol from five *Nepeta* species

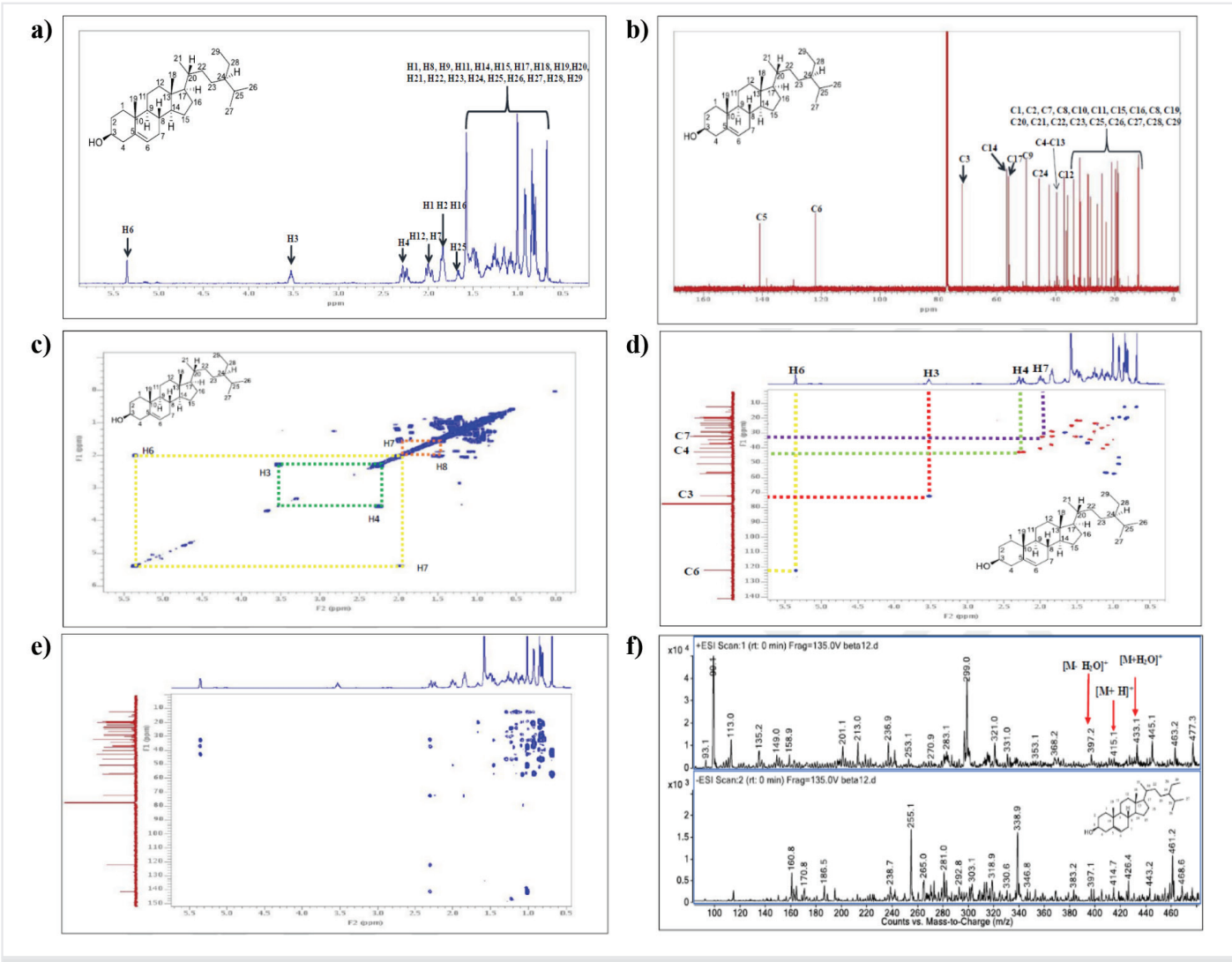

Figure 2. a) ^{1}H-NMR (CD_3OD, 600 MHz), b) ^{13}C-NMR (CD_3OD, 150 MHz, c) COSY, d) HSQC, e) HMBC spectra, (f) MS spectra of the β-sitosterol

the active site of the urease enzyme (Supplementary Table 1 and Figure 4a). The interactions of the BS with urease, binding affinities, and constant (-7.50 kcal/mol and 3.86 μM) were calculated (Table 2).

Eight alkyl connections with ALA65, ILE91, VAL121, and LEU198, as well as six P-A contacts with HIS94, HIS96, and PHE131, were generated by BS, which interacts with the active region of the CA enzyme (Supplementary Table 2 and Figure 4b). The interactions of the BS with CA, binding affinities, and constant (-7.40 kcal/mol and 3.71 μM) were determined (Table 2).

The lipase enzyme's active site is where BS interacts. It was shown to form one P-A contact with HIS354, two carbon-hydrogen bonds with ASP272 and LYS268, four alkyl interactions with LYS268 and LEU356, and one conventional hydrogen bond with ASP272 (Supplementary Table 3 and Figure 4c). Interactions of BS with lipase, binding affinities, and constants (-7.00 kcal/mol and 11.54 μM) were calculated (Table 2).

According to Supplementary Table 4 and Figure 5a, BS interacts with the tyrosinase enzyme's active site by forming eight alkyl contacts with ALA228 and VAL300 and five P-A interactions with PHE239, TYR297, and PHE537. The interactions of the BS with tyrosinase, with a binding affinity and constant (-8.80 kcal/mol and 0.62 μM), were calculated (Table 2).

According to Supplementary Table 5 and Figure 5b, BS interacts with the α-amylase enzyme's active site by forming one hydrogen bond with ALA3, nine alkyl contacts with ALA3, LEU211, ARG227, PRO228, ILE230, and LYS208, and one P-A interaction with TYR2. The interactions of the BS with α-amylase to have a binding affinity and constant (-8.90 kcal/mol and 0.53 μM), were calculated (Table 2).

Supplementary Table 6 and Figure 5c show that BS interacts

Table 1. ^{1}H- and ^{13}C-NMR data and literature values of the β-sitosterol

No	^{1}H-NMR ((CD_3OD, 600 MHz)	^{13}C-NMR (CD_3OD, 150 MHz)	^{1}H-NMR (22)	^{13}C-NMR (22)
1	1.07-1.84 (m)	37.23	1.46 (m)	37.28
2	1.50-1.83 (m)	31.64	1.56 (m)	31.69
3	3.51	71.8	3.54	71.82
4	2.25-2.28 (m)	42.28	2.32 (m)	42.33
5	-	140.70	-	140.77
6	5.34	121.25	5.37	121.73
7	1.97	31.9	2.04	31.93
8	1.44	31.88	1.69	31.93
9	0.93	50.1	1.55	50.16
10	-	36.49	-	36.51
11	1.48	21.07	1.52	21.11
12	1.15-1.99 (m)	39.75	1.51 (m)	39.80
13	-	42.30	-	42.34
14	0.98	56.75	1.50	56.79
15	1.57	24.29	1.58	24.33
16	1.83	28.24	1.85	28.27
17	1.1	56.02	1.45	56.08
18	0.84	11.85	0.7	11.89
19	1.0	19.39	1.03	19.42
20	1.35	36.13	1.6	36.17
21	0.91	18.77	0.94	18.84
22	1.0-1.31 (m)	33.92	0.93 (m)	33.98
23	1.15	26.02	1.15	26.11
24	0.92	45.80	1.38	45.86
25	1.65	29.11	1.57	29.19
26	0.82	19.82	0.84	19.84
27	0.8	19.01	0.86	19.06
28	1.21-1.26 (m)	23.04	1.12 (m)	23.10
29	0.67	11.97	0.82	12.01

NMR: Nuclear magnetic resonance

with the active site of the α-glucosidase enzyme by forming one alkyl contact with PRO82 and one P-A interaction with TRP81. The interactions of the BS with α-glucosidase, with a binding affinity and constant of -8.00 kcal/mol and 2.27 μM, were calculated (Table 2).

Molecular Dynamics (MD) Simulations

In drug development methods, analyzing the dynamic behavior of molecules and the complex systems in which these molecules interact is indispensable. MD simulation is one of the calculations made in a computer environment. MD simulations enable the determination of flexibility in targets that traditional molecular docking techniques cannot. This way, the calculated binding energies can provide more accurate information about potential inhibitors (24).

Since it was observed that BS had the best interaction with tyrosinase in our molecular docking studies, enzyme kinetics, and inhibition studies, an MD simulation was performed on the complex it formed with tyrosinase. RMSD, RMSF, Rg values, and H-bonds were utilized in MD simulations to assess the stability of BS under physiological conditions in the presence of tyrosinase. From the RMSD plots, the complexes remained stable for 100 ns at approximately 4-4.5 nm (Figure 6a). During the simulation, RMSF calculates the changes in amino acid residues in the absence of ligand molecules. According to Figure 6b, the calculated RMSF values for tyrosinase indicate that the intensity of the fluctuation ranges from 0.05 to 0.40 nm. The H-bonds generated by the complexes at 100 ns in the MD simulation are shown in Figure 6c. The MD simulation showed that one to three H-bonds interacted in both complexes.

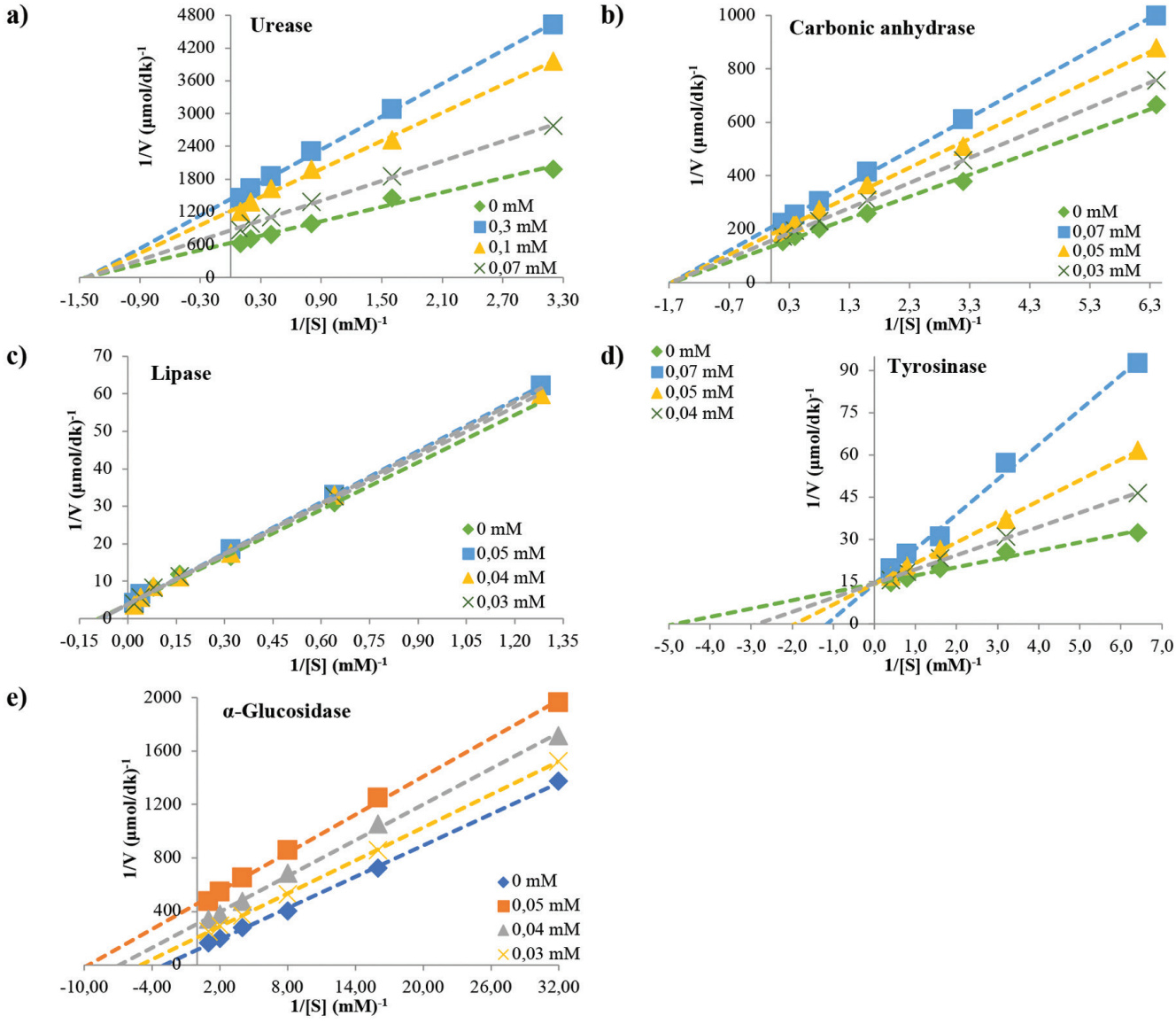

Figure 3. Lineweaver-Burk plots of a) urease, b) carbonic anhydrase, c) lipase, d) tyrosinase, and e) α-glucosidase for β-sitosterol

Rg shows the loose molecular packing of a protein and is a valuable and accurate indicator of a drug's ability to alter protein structure. The dynamic calculation for 100 ns in Figure 6d shows that tyrosinase and BS are coherent at about 2.40 and 0.50 nm.

MM/PBSA analysis

The binding free energy may be found using MM/PBSA, one of the most commonly used methods. One can expect that a ligand-protein combination is more stable and has more ligand activity and potency if its estimated free binding energy is lower. Protein-ligand complexes' free binding energy ($\Delta G_{binding}$) was assessed using MM-PBSA. The energy contributions are G_{GAS} and G_{SOLV}, and MM-PBSA is ranked using the binding energy parameters. E_{GB} and E_{SURF} are the polar and non-polar contributions, according to the GB estimations in Table 3. Despite the considerable electrostatic contribution of all mutations, the van der Waals term is the primary contributor to the overall binding free energy, as it is significantly offset by a large positive polar contribution (E_{GB}). The overall polar contribution (E_{EL}+E_{GB}) is thus positive (25). The complexes' ΔG binding values for tyrosinase are -4.39 kcal/mol, as shown in Figure 6e. An examination of the MM-PBSA data showed that the van der Waals contact force is far more significant than the electrostatic force in protein-ligand interaction. The MD simulation's output parameters and the docking findings exhibit a significant correlation, suggesting that the docked protein-ligand complexes remain stable during the simulation.

Table 2. Enzyme inhibitions, inhibition types, binding affinities and constants of *β*-sitosterol

Enzymes	β-sitosterol	Standard drugs	Inhibition types	Inhibitor constant (K_i, μM)	Binding affinity (kcal/mol)	Binding constant (K_i, μM)
	IC_{50} (μM)					
Urease	21.60±0.01	130.98±0.00 (Thiourea)	Non-competitive	335.55	-7.50	3.86
CA	67.70±0.01	10.57±0.27 (Acetazolamide)	Non-competitive	203.40	-7.40	3.71
Lipase	42.50±0.02	12.71±2.04 (Orlistat)	Competitive	1032.22	-7.00	11.54
Tyrosinase	6.60±0.02	181.76±11.12 (Kojic acid)	Competitive	37.35	-8.80	0.62
α-amylase	280.09±0.00	40.16±0.25 (Acarbose)	-	-	-8.90	0.53
α-glucosidase	274.64±6.80	20.91±0.06 (Acarbose)	Uncompetitive	25.67	-8.00	2.27

IC_{50}: Half-maximal drug inhibitory concentration, K_i: Inhibitor constant, CA: Carbonic anhydrase

Discussion

Enzyme Inhibitions and Kinetic Assays

In the literature search, no references were found to compare the inhibition and inhibition kinetics of urease, CA, and lipase. For this reason, the study on these enzymes will be the first. In previous studies, the α-amylase inhibition of BS was found to be 0.21±0.01 mmol ACAE/g IC_{50} value of 154.40±15.80 μg/mL (26), and an IC_{50} value of 55.25 μg/mL (27). In another study, the inhibition of α-amylase by BS could not be determined (28). When the results in the literature are compared with those in our study, the α-amylase inhibition in our study is lower.

Sheng et al. (27) determined the type of α-amylase inhibition by BS as semi-competitive and the K_i value as 5.51 μg/mL.

In previous studies, the α-glucosidase inhibition of BS was found to be 14.69±0.15 mmol ACAE/g (29), an IC_{50} value >100 μg/mL Salah El Dine et al. (30), and an IC_{50} value of 283.67 μg/mL (27). In another study, α-glucosidase inhibition of BS could not be determined (28). The results of our investigation indicate a lower level of α-glucosidase inhibition compared to those reported in the literature.

Sheng et al. (31) determined that the inhibition type of α-glucosidase by BS was competitive, with a K_i value of 20.09 mg/L. In contrast, another study by Sheng et al. (27) determined that the inhibition type of α-glucosidase by BS was non-competitive, with a K_i value of 20.09 μg/mL.

In previous studies, the tyrosinase inhibition of BS was found to be 8.10±0.24 mg KAE/g (26), 73.42±1.67 mg KAE/g (29), 73.42±1.67 mg KAE/g (32), and in another study, the tyrosinase inhibition of BS could not be determined (33).

Molecular Docking

Quek et al. (26) calculated the binding energy of the BS-α-amylase interaction as -9.30 kcal/moL. In our study, the binding energy of the BS-α-amylase interaction was observed to be higher. Hasan et al. (34) determined the docking score of the BS-α-amylase interaction as -3.21, and Purnomo et al. (35) calculated the binding energies of the α-amylase and α-glucosidase interaction of BS as -8.66 and -9.59 kcal/mol. In our study, the binding energy of the BS-α-amylase interaction was lower, whereas the binding energy of the α-glucosidase interaction was higher. Mandar et al. (36) found the binding energies of the α-amylase and α-glucosidase interactions with BS to be -9.30 and -8.50 kcal/mol, respectively. In our study, the binding energies of the α-amylase and α-glucosidase interaction of BS were observed to be higher. In the study conducted by Shanak et al. (37), the binding energies of the interaction of BS with α-amylase and α-glucosidase were observed as -8.38 kcal/mol, -7.93 kcal/mol, and the binding constants as 719.79 nM, 1.53 μM. In our study, the binding energies of the interaction of BS with α-amylase and α-glucosidase were observed to be lower. Sari et al. (38) determined the binding energy of the interaction of BS and α-glucosidase as -10.61 kcal/mol. In our study, the binding energy of the interaction of BS-α-glucosidase was determined to be lower.

Study Limitations

The fact that there are many previous enzyme inhibition studies on BS is a limitation of this study.

Conclusion

Our study investigated the enzyme inhibition activities and kinetics of BS isolated from five different *Nepeta* species (*N. aristata, N. italica, N. baytopii, N. stenantha,* and *N. trachonitica*). In addition, the molecular structure of BS was determined using NMR, and its mass was determined using MS. It was recorded that BS had high urease and tyrosinase inhibition. The enzyme inhibition kinetics of BS with urease, CA, lipase, tyrosinase, α-amylase, and α-glucosidase were investigated, and the inhibitory constant formed by urease and tyrosinase was high. Upon examining the molecular docking, it was observed that α-amylase exhibited the highest binding affinity among the six enzymes. Considering these results, the MD simulation of BS with tyrosinase was investigated. It was observed to be stable at 4 nm for 100 ns in the RMSD graph. Additionally, the binding energy was calculated to be -4.39 kcal/mol using MM/PBSA analysis. Thus, it is likely to play a leading role in the use of cosmetics and drugs.

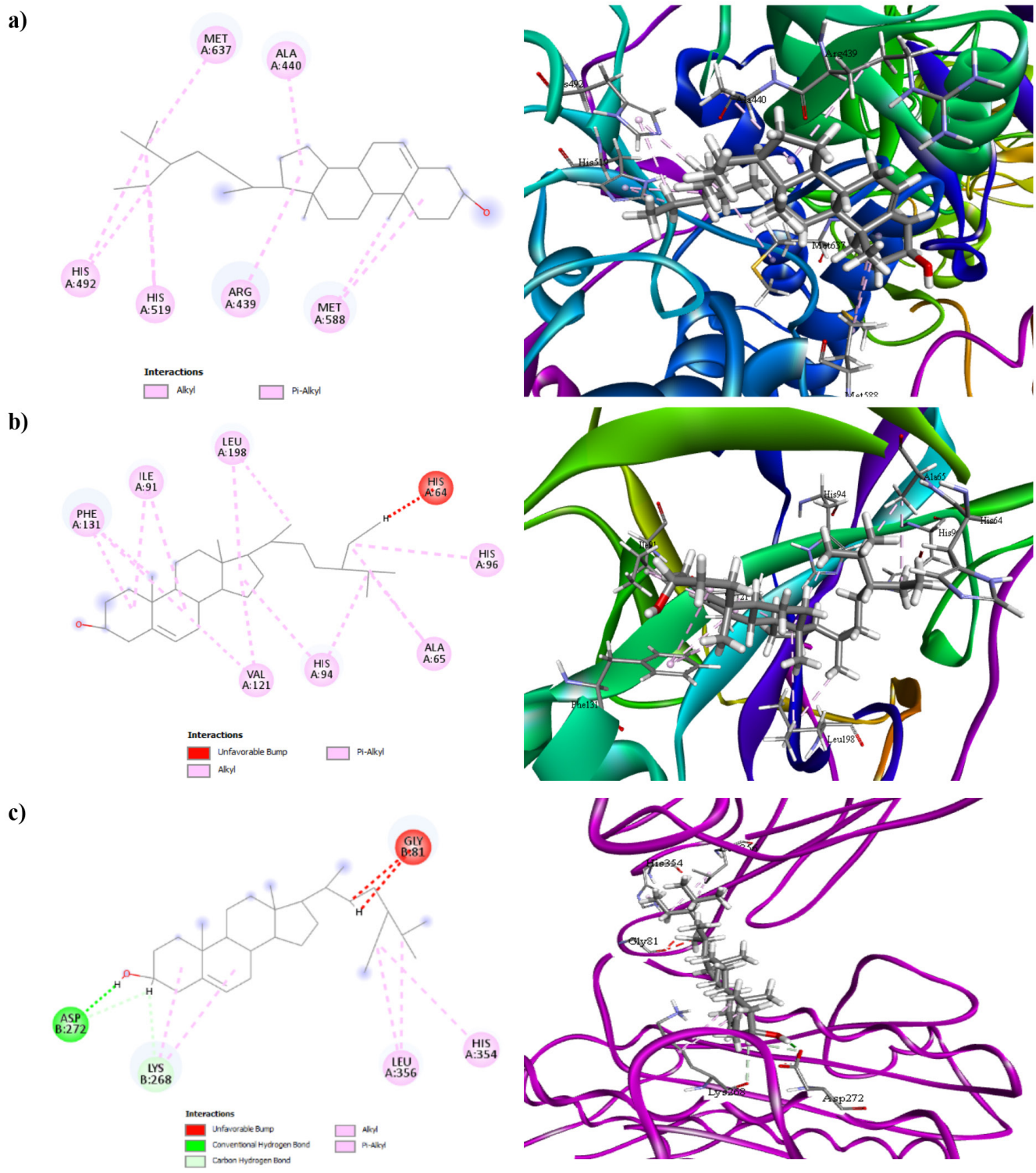

Figure 4. Molecular docking 2D and 3D images of the β-sitosterol a) urease, b) CA, and c) lipase

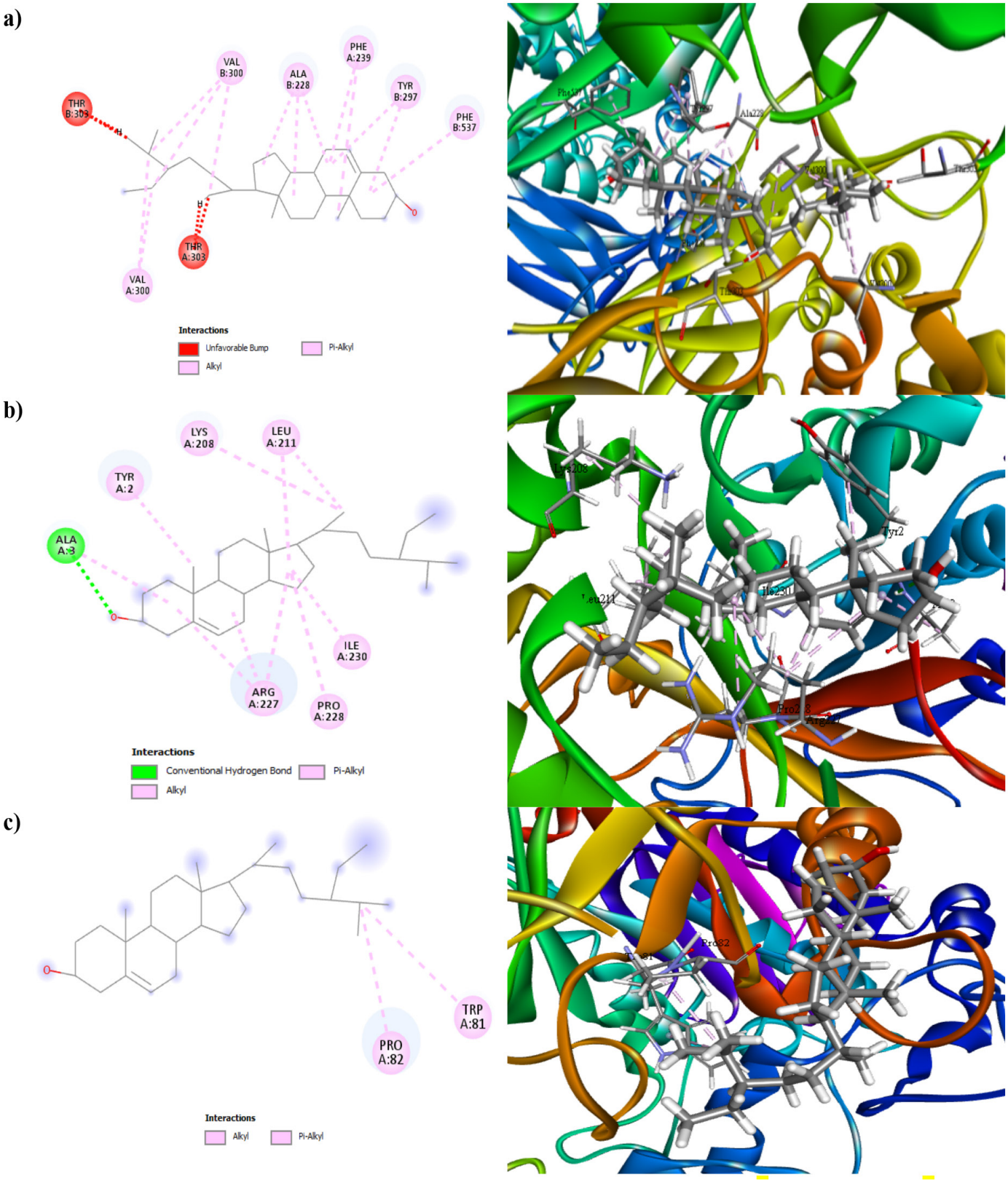

Figure 5. Molecular docking 2D and 3D images of the β-sitosterol a) tyrosinase, b) α-amylase, and c) α-glucosidase

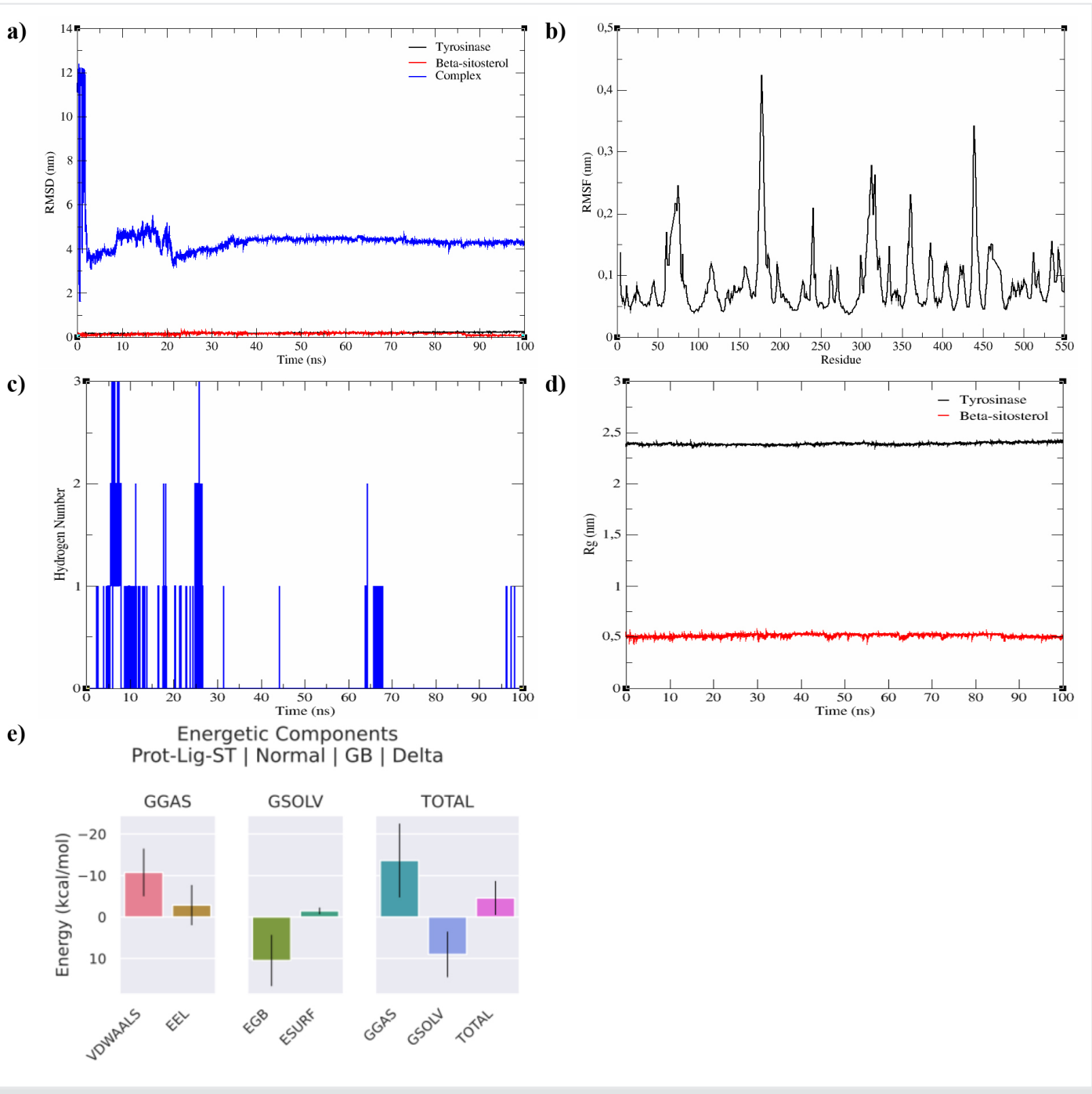

Figure 6. a) RMSD and b) RMSF, c) H-bond interactions, d) Rg plotting, e) MM-PBSA energy with tyrosinase

RMSD: Root mean square deviation, RMSF: Root-mean-square fluctuation, Rg: Radius of gyration, E_{EL}: Electrostatic energy as calculated by the MM force field, E_{GB}: The electrostatic contribution to the solvation-free energy calculated by GB, E_{SURF}: Hydrophobic contribution to solvation-free energy for GB calculations, G_{SOLV}: Sum of nonpolar and polar contributions to solvation, G_{GAS}: Total gas phase energy (ELE+VDW+INT)

Table 3. MM/PBSA energy results of the complex

Compounds	VDW	E_{EL}	E_{GB}	E_{SURF}	ΔG_{GAS}	ΔG_{SOLV}	$\Delta G_{binding}$
β-sitosterol-tyrosinase	-7.21±6.92	-7.71±10.03	11.73±11.87	-1.20±1.17	-14.93±15.52	10.54±10.82	-4.39±5.13

MM/PBSA: Molecular mechanics Poisson-Boltzmann surface area, VDW: Van der Waals contribution from MM, E_{EL}: Electrostatic energy as calculated by the MM force field, E_{GB}: The electrostatic contribution to the solvation-free energy calculated by GB, E_{SURF}: Hydrophobic contribution to solvation-free energy for GB calculations, ΔG_{GAS}: Total gas phase energy (ELE+VDW+INT), ΔG_{SOLV}: Sum of non-polar and polar contributions to solvation, $\Delta G_{binding}$: Final estimated binding free energy calculated from the terms above (kcal/mol)

Ethics

Ethics Committee Approval: Not obtained, as no animals or humans were used in the study. Additionally, our study does not require approval from an ethics committee.

Informed Consent: Not obtained, as no patients were involved in the study. Additionally, our study does not require patient consent.

Footnotes

Authorship Contributions

Surgical and Medical Practices: S.Y., Y.B., I.D., T.O., Concept: S.Y., Y.B., Y.I., I.D., T.O., L.B., Design: S.Y., Y.B., Y. I., I.D., T. O., L.B., Data Collection or Processing: S.Y., Y.B., I.D., T.O., Analysis or Interpretation: S.Y., Y.B., Y. I., I.D., T.O., Literature Search: S.Y., Y.B., I.D., T.O., Writing: S.Y., Y.B., I.D., T.O.

Conflict of Interest: No conflict of interest was declared by the authors.

Financial Disclosure: We thank TÜBİTAK (The Scientific and Technological Research Council of Türkiye) for financial support (project number: 119Z442).

Supplementary Tables 1-6: https://d2v96fxpocvxx.cloudfront.net/bd1986e1-0bc1-4f4d-af66-3a184850a065/content-images/4f6b5280-110e-4a31-913f-3b2d7fd6bf95.pdf

References

1. Shoker R. A review article: the importance of the major groups of plants secondary metabolism phenols, alkaloids, and terpenes. Int J Res Appl Sci Biotechnol. 2020;7:354-8.
2. Erenler R, Telci I, Ulutas M, Demirtas I, Gul F, Elmastas M, et al. Chemical constituents, quantitative analysis and antioxidant activities of *Echinacea purpurea* (L.) Moench and *Echinacea pallida* (Nutt.) Nutt. Journal of Food Biochemistry. 2015;39:622-30.
3. Yenigün S, Başar Y, İpek Y, Behçet L, Özen T, Demirtaş İ. Determination of antioxidant, DNA protection, enzyme inhibition potential and molecular docking studies of a biomarker ursolic acid in *Nepeta* species. J Biomol Struct Dyn. 2024;42:5799-816.
4. Patel H, Gomes EN, Yuan B, Lyu W, Wu Q, Simon JE. Investigation of volatile iridoid terpenes in *Nepeta cataria* L. (Catnip) Genotypes. Molecules. 2022;27:7057.
5. Garg A, Sharma R, Dey P, Kundu A, Kim HS, Bhakta T, et al. Chapter 11 - analysis of triterpenes and triterpenoids. In: Sanches Silva A, Nabavi SF, Saeedi M, Nabavi SM, editors. Recent Advances in Natural Products Analysis: Elsevier; 2020. p.393-426.
6. Saeidnia S, Manayi A, Gohari A, Abdollahi M. The story of beta-sitosterol- a review. European J Med Plants. 2014;4:590-609.
7. Panda P, Dash P, Ghosh G. Chemometric profile, antioxidant and tyrosinase inhibitory activity of Camel's foot creeper leaves (Bauhinia vahlii). Nat Prod Res. 2018;32:596-9.
8. Bin Sayeed MS, Karim SMR, Sharmin T, Morshed MM. Critical analysis on characterization, systemic effect, and therapeutic potential of beta-sitosterol: a plant-derived orphan phytosterol. Medicines (Basel). 2016;3:29.
9. Han NR, Kim HM, Jeong HJ. The β-sitosterol attenuates atopic dermatitis-like skin lesions through down-regulation of TSLP. Exp Biol Med (Maywood). 2014;239:454-64.
10. Kim SJ. The ameliorative effect of β-sitosterol on DNCB-induced atopic dermatitis in mice. Biomed Sci Lett. 2017;23:303-9.
11. Başar Y, Yenigün S, İpek Y, Behçet L, Gül F, Özen T, et al. DNA protection, molecular docking, enzyme inhibition and enzyme kinetic studies of 1,5,9-epideoxyloganic acid isolated from *Nepeta aristata* with bio-guided fractionation. J Biomol Struct Dyn. 2024;42:9235-48.
12. Yenigun S, Basar Y, Ipek Y, Behcet L, Demirtas I, Ozen T. DNA protection, molecular docking, molecular dynamic, enzyme inhibition, and kinetics studies of apigenin isolated from *Nepeta baytopii* Hedge & Lamond by bioactivity-guided fractionation. J Biomol Struct Dyn. 2025;43:9404-15.
13. İpek Y, Başar Y, Yenigün S, Behçet L, Özen T, Demirtaş İ. *In vitro* bioactivities and *in silico* enzyme interactions of abietatrien-3*β*-ol by bio-guided isolation from *Nepeta italica* subsp. *italica*. J Biomol Struct Dyn. 2025;43:7649-72.
14. Zhang L, Mulrooney SB, Leung AF, Zeng Y, Ko BB, Hausinger RP, et al. Inhibition of urease by bismuth(III): implications for the mechanism of action of bismuth drugs. Biometals. 2006;19:503-11.
15. Chanda J, Mukherjee PK, Biswas R, Biswas S, Tiwari AK, Pargaonkar A. UPLC-QTOF-MS analysis of a carbonic anhydrase-inhibiting extract and fractions of *Luffa acutangula* (L.) Roxb (ridge gourd). Phytochemical Analysis. 2019;30:148-55.
16. Addar L, Bensouici C, Zennia SSA, Haroun SB, Mati A. Antioxidant, tyrosinase and urease inhibitory activities of camel αS-casein and its hydrolysate fractions. Small Ruminant Research. 2019;173:30-5.
17. Yang XW, Huang MZ, Jin YS, Sun LN, Song Y, Chen HS. Phenolics from *Bidens bipinnata* and their amylase inhibitory properties. Fitoterapia. 2012;83:1169-75.
18. Mayur B, Sandesh S, Shruti S, Sung Yum S. Antioxidant and α-glucosidase inhibitory properties of *Carpesium abrotanoides* L. J Med Plants Res. 2010;4:1547-53.
19. Trentin R, Custódio L, Rodrigues MJ, Moschin E, Sciuto K, da Silva JP, et al. Exploring Ulva australis Areschoug for possible biotechnological applications: in vitro antioxidant and enzymatic inhibitory properties, and fatty acids contents. Algal Research. 2020;50:101980.
20. Başar Y, Demirtaş İ, Yenigün S, İpek Y, Özen T, Behçet L. Molecular docking, molecular dynamics, MM/PBSA approaches and bioactivity studies of nepetanudoside B isolated from endemic *Nepeta aristata*. J Biomol Struct Dyn. 2025;43:5486-99.
21. Kumari R, Kumar R; Open Source Drug Discovery Consortium; Lynn A. g_mmpbsa--a GROMACS tool for high-throughput MM-PBSA calculations. J Chem Inf Model. 2014;54:1951-62.
22. Ododo MM, Choudhury MK, Dekebo AH. Structure elucidation of β-sitosterol with antibacterial activity from the root bark of Malva parviflora. Springerplus. 2016;5:1210.
23. Hopkins AL, Groom CR. The druggable genome. Nat Rev Drug Discov. 2002;1:727-30.

24. Liu X, Shi D, Zhou S, Liu H, Liu H, Yao X. Molecular dynamics simulations and novel drug discovery. Expert Opin Drug Discov. 2018;13:23-37.
25. Gautam V, Nimmanpipug P, Zain SM, Rahman NA, Lee VS. Molecular dynamics simulations in designing DARPins as phosphorylation-specific protein binders of ERK2. Molecules. 2021;26:4540.
26. Quek A, Kassim NK, Lim PC, Tan DC, Mohammad Latif MA, Ismail A, et al. α-Amylase and dipeptidyl peptidase-4 (DPP-4) inhibitory effects of *Melicope latifolia* bark extracts and identification of bioactive constituents using *in vitro* and *in silico* approaches. Pharm Biol. 2021;59:964-73.
27. Sheng Z, Dai H, Pan S, Ai B, Zheng L, Zheng X, et al. Phytosterols in banana (*Musa spp.*) flower inhibit α-glucosidase and α-amylase hydrolysations and glycation reaction. International Journal of Food Science & Technology. 2017;52:171-9.
28. Torres-Naranjo M, Suárez A, Gilardoni G, Cartuche L, Flores P, Morocho V. Chemical constituents of Muehlenbeckia tamnifolia (Kunth) Meisn (Polygonaceae) and its in vitro α-amilase and α-glucosidase inhibitory activities. Molecules. 2016;21:1461.
29. Akramov DK, Bacher M, Böhmdorfer S, Rosenau T, Zengin G, Potthast A, et al. Phytochemical analysis and biological evaluation of *Lagochilus* species from Uzbekistan. Industrial Crops and Products. 2020;154:112715.
30. Salah El Dine R, Ma Q, Kandil ZA, El-Halawany AM. Triterpenes as uncompetitive inhibitors of α-glucosidase from flowers of Punica granatum L. Nat Prod Res. 2014;28:2191-4.
31. Sheng Z, Dai H, Pan S, Wang H, Hu Y, Ma W. Isolation and characterization of an α-glucosidase inhibitor from Musa spp. (Baxijiao) flowers. Molecules. 2014;19:10563-73.
32. Sut S, Dall'Acqua S, Sinan KI, Bene K, Kumar G, Mahomoodally MF, et al. Cola caricifolia (G. Don) K. Schum and Crotalaria retusa L. from Ivory Coast as sources of bioactive constituents. Ind Crops Prod. 2020;147:112246.
33. Balur Adsız L. *Salvia cerino-pruinosa* var. *elazigensis* türünün antioksidan aktivite kontrollü sekonder metabolit izolasyonu (dissertation). Diyarbakır: Dicle Üniversitesi. 2018.
34. Hasan M, Kabir MSH, Mojumder M, Paul A, Rahman MR, Akter Y, et al. *In silico* molecular docking studies of some isolated compounds from *Nauclea latifolia* for α-amylase inhibitory activity and ADME/T property analysis of the compounds. World J Pharm Res. 2016;5:1742-50.
35. Purnomo Y, Makdasari J, Fatahillah FI. Inhibitory activity of *Urena lobata* leaf extract on alpha-amylase and alpha-glucosidase: *in vitro* and *in silico* approach. J Basic Clin Physiol Pharmacol. 2021;32:889-94.
36. Mandar BK, Khanal P, Patil BM, Dey YN, Pasha I. In silico analysis of phytoconstituents from *Tinospora cordifolia* with targets related to diabetes and obesity. In Silico Pharmacol. 2021;9:3.
37. Shanak S, Bassalat N, Albzoor R, Kadan S, Zaid H. *In vitro* and *in silico* evaluation for the inhibitory action of *O. basilicum* methanol extract on *α*-glucosidase and *α*-amylase. Evid Based Complement Alternat Med. 2021;2021:5515775.
38. Sari BL, Mun'im A, Yanuar A, Riadhi R. Screening of a-glucosidase inhibitors from Terminalia catappa L. fruits using molecular docking method and in vitro test. Int J Pharm Pharm Sci. 2016;8:184-9.